

# Human-in-the-loop Adaptation in Group Activity Feature Learning for Team Sports Video Retrieval

Chihiro Nakatani<sup>a</sup>, Hiroaki Kawashima<sup>b</sup>, Norimichi Ukita<sup>a</sup>

<sup>a</sup>*Toyota Technological Institute, 2-12-1 Hisakata, Tempaku-ku, Nagoya, 468-8511, Aichi, Japan*

<sup>b</sup>*University of Hyogo, 8-2-1 Gakuennishi-machi, Nishi-ku, Kobe, 651-2197, Hyogo, Japan*

## Abstract

This paper proposes human-in-the-loop adaptation for Group Activity Feature Learning (GAFL) without group activity annotations. This human-in-the-loop adaptation is employed in a group-activity video retrieval framework to improve its retrieval performance. Our method initially pre-trains the GAF space based on the similarity of group activities in a self-supervised manner, unlike prior work that classifies videos into pre-defined group activity classes in a supervised learning manner. Our interactive fine-tuning process updates the GAF space to allow a user to better retrieve videos similar to query videos given by the user. In this fine-tuning, our proposed data-efficient video selection process provides several videos, which are selected from a video database, to the user in order to manually label these videos as positive or negative. These labeled videos are used to update (i.e., fine-tune) the GAF space, so that the positive and negative videos move closer to and farther away from the query videos through contrastive learning. Our comprehensive experimental results on two team sports datasets validate that our method significantly improves the retrieval performance. Ablation studies also demonstrate that several components in our human-in-the-loop adaptation contribute to the improvement of the retrieval performance. Code: <https://github.com/chihina/GAFL-FINE-CVIU>.

**Keywords:** Group activity feature learning, Fine-tuning, Human-in-the-loop, Team sports video retrieval,

## 1. Introduction

Group activities are characterized by multiple people engaging in interactions within the same group. The group activities are important cues for team sports analysis. Group Activity Recognition (GAR) is a task to classify a frame or a video into predefined group activity classes [1, 2, 3, 4, 5, 6, 7, 8, 9, 10, 11, 12, 13, 14, 15, 16, 17, 18, 19, 20, 21]. These GAR methods are trained in a supervised manner, which requires a large number of ground-truth group activity annotations, as shown in Fig. 1 (a).

Annotating group activities is more challenging than a single person's actions. In a single person's action recognition, AI-driven wearable systems [22] allow for constant tracking of the target person's activity. However, group activities with a large number of group people (e.g., 12 and 10 in volleyball and basketball, respectively) make the annotations more labor-intensive and less reliable. Furthermore, to apply GAR to complex real-world applications (e.g., team sports analysis), it is not easy to appropriately pre-define all group activities as follows: (1) complex interactions among people make it difficult to define all group activities necessarily and sufficiently and (2) the

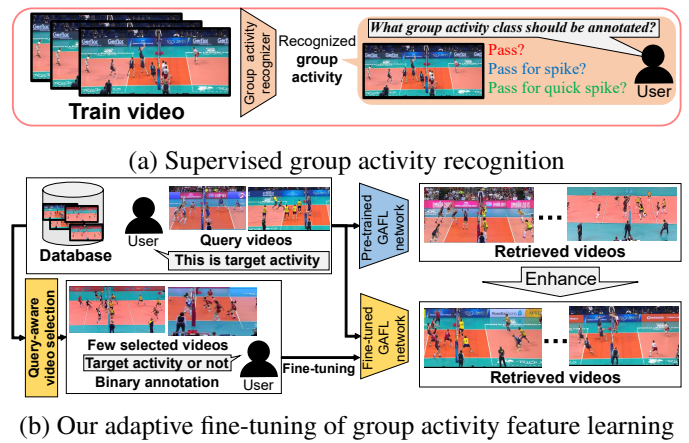


Figure 1: Difference between previous method and our method. (a) Supervised GAR employs group activity annotations that are difficult due to various similar group activities. (b) Our proposed method adaptively fine-tunes the pre-trained GAF space for retrieving target group activity represented by query videos given by users. Our fine-tuning only requires binary annotations to users on a few selected videos, eliminating group activity annotations.

necessary and sufficient classes of group activities may differ depending on various factors (e.g., users, scenarios, times, and applications). For example, 200 or more plays are defined every year in American Football games [23, 24, 25].

To avoid these difficulties in annotating group activities, Group Activity Feature Learning (GAFL) [26] trains Group Activity Features (GAFs) in a self-supervised manner without

group activity annotations. While GAFL provides no group activity classes unlike supervised GAR, the trained GAF is directly applicable to video retrieval from a video database. This retrieval is useful for strategy and tactics analysis in team sports. For example, retrieving videos that show a specific spike pattern leading to points can help tactics analysis.

However, GAF trained only with a self-supervised manner is still insufficient. For example, the GAF trained by GAFL on the Volleyball dataset [27] is visualized in Fig. 2 with t-SNE [28]. In this example, the color of each point corresponds to its manually annotated group activity label. This visualization reveals that the learned GAF is not enough to discriminate between group activities, as many points with different colors are mixed.

To improve GAFL, our method incorporates human-in-the-loop adaptation with GAFL. Our method fine-tunes the GAF space, which was pre-trained in a self-supervised manner. This fine-tuning aims to better retrieve videos similar to user-provided query videos in a human-in-the-loop manner (Fig. 1 (b)). The user simply provides a few query videos with no annotations of group activity labels. This approach avoids the need to define group activity classes linguistically and semantically, which are inherently complex as mentioned above.

Using the query videos, our proposed video selection process chooses several videos from a video database. Unlike general uncertainty-based selection in active learning [29, 30, 31], this paper proposes query-aware video selection specifically designed for Group Activity Retrieval (GARet). The user annotates whether these selected videos are what to expect as group activity videos or not (i.e., positive or negative). That is, different from supervised GAR methods where annotators need to classify a large number of training videos into many complex group activity classes, our method simply and directly requires the user to judge whether or not each selected video matches their target group activity videos. Finally, the GAF space is fine-tuned by the annotated selected videos to improve the GAF discriminability on videos similar to the users’ query videos.

Since the user demands (e.g., what kind of spike patterns are required) vary on a case-by-case basis, retrieving a particular target group activity is essential. In terms of the user experience and usability in sports analysis applications, the amount of video annotations should be minimal. Thus, our human-in-the-loop adaptation requests the user to label only a limited number of selected videos (e.g., five) once as positive or negative.

For example, our human-in-the-loop adaptation supports a use case as follows: (i) an analyst provides a few query videos representing the target group activity, such as sample videos in which the team gets a point; (ii) the analyst annotates videos selected from a database of past plays; and (iii) the analyst receives retrieved videos from the fine-tuned GAF model to analyze tactics leading to points based on many videos.

Our novel contributions are summarized as follows:

- **Human-in-the-loop adaptation in GAFL:** This paper proposes a human-in-the-loop adaptation scheme for GARet. In this scheme, a pre-trained GAF space [26] is updated to improve the discriminativeness of a target group activity without group activity annotations.

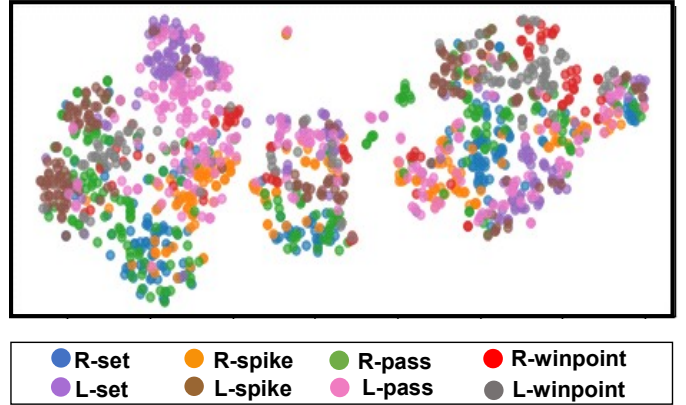


Figure 2: Group activity feature space learned by [26] in a self-supervised manner on the Volleyball dataset [27]. The group activity feature extracted from each video is transformed into 2-dimensional features by t-SNE [28]. The color of each point corresponds to its group activity label annotated in the Volleyball dataset. While the manually annotated group activity labels are not used for the training, the group activity labels are only used for the visualization in this figure. The visualization reveals that group activity features are not learned enough in [26] to discriminate between the different group activities.

- **Query-aware video selection for fine-tuning:** For data-efficient fine-tuning, this paper proposes video selection using query videos.

**Query similarity:** To select videos similar to query videos in terms of group activities, we select videos that are close to one of the query videos in the GAF space. Unlike active learning [29, 30, 31] using only the uncertainty of each unlabeled sample, we focus on the similarity between unlabeled videos and query videos to learn subtle distinctions between target and other group activities.

**Query local dissimilarity:** Sample video selection only with the above query similarity may select too similar videos, leading to inefficient fine-tuning. To avoid this problem, in evaluating the similarity between the query and sample videos, several people are masked to assess local dissimilarity (i.e., similarity of some people). Sample video selection using this local dissimilarity in conjunction with the aforementioned query similarity (i.e., similarity of all people) allows us to select globally similar but locally dissimilar videos.

- **Comprehensive evaluation:** We conduct comprehensive experiments on team sports datasets (i.e., volleyball [27] and basketball [14]) to validate the applicability of our method in the team sports domain. Ablation studies also demonstrate that our method efficiently updates the pre-trained GAF space for the target group activity.

## 2. Related Work

### 2.1. Group Activity Recognition (GAR)

In [7, 12, 17, 21, 32], manual group activity annotations are used for training GAR models. In [12], a group activity is recognized from a whole image. In [32], human poses and object

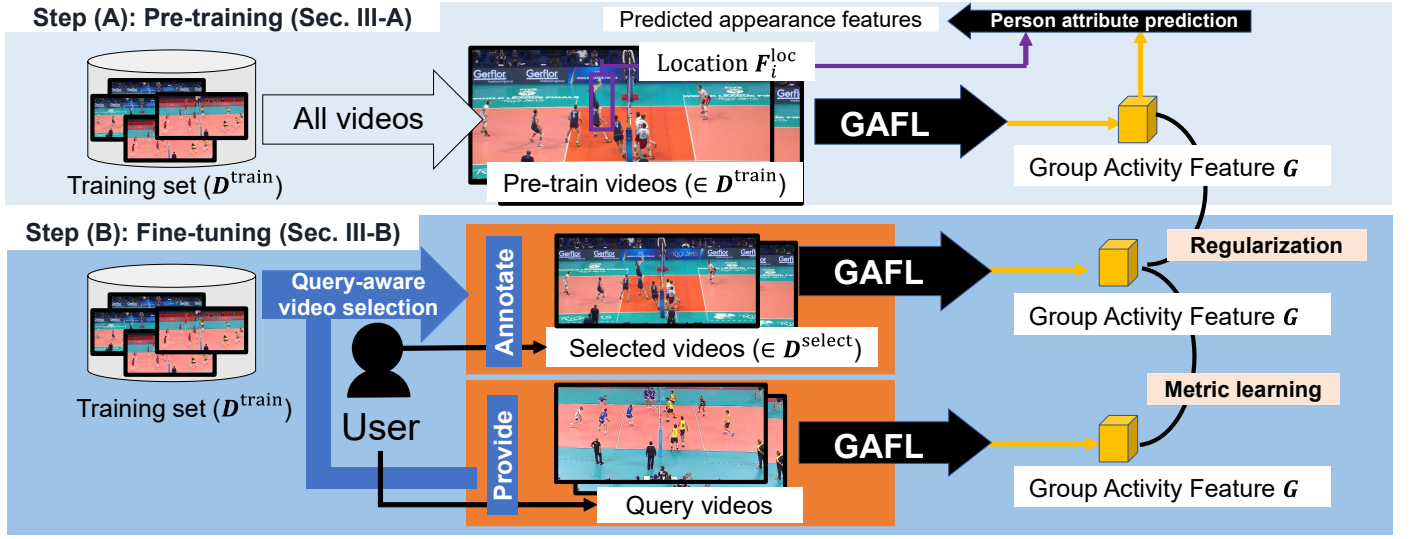


Figure 3: Overview of our proposal. (a) group activity feature learning network is pre-trained by [26] with the training dataset. (b) The pre-trained group activity feature learning network is fine-tuned for target group activity presented by query videos given by users.

keypoints are fed into a group activity recognizer in which interaction between multi-person and object is built as a graph. The set of person features is employed for a Graph Neural Network (GNN) by Kim *et al* [7] and Yan *et al* [17] as well as [2, 5]. In [6, 8, 9, 10, 11, 20], Transformer [33] improves the interaction modeling using a self-attention mechanism. In [21], an optical flow map is used to guide attention maps in the transformer encoder to focus on foreground objects.

Different from these GAR methods that are trained with pre-defined group activity annotations, our method fine-tunes a pre-trained GAF space based on any target group activity represented by query videos given by users.

## 2.2. Group Activity Feature Learning (GAFL)

While general representation learning methods extract low-level features for various downstream tasks such as general image/video classification and prediction, several representation learning methods [1, 26] focus on high-level group activity features extracted from multiple people for group-related tasks (e.g., group scene retrieval and clustering). In [1], scene features of multiple people are learned in a self-supervised manner through GNN. Nakatani *et al.* [26] also aims to extract the features of multiple people in a self-supervised manner through person attribute prediction as a pretext task.

In our method, any pre-trained GAF space provided by these self-supervised methods [26] is fine-tuned with human feedback for the retrieval task. The domain-specific adaptation of existing frameworks that we propose is novel, similar to how Awad *et al* [34] have yielded novel contributions within existing recognition frameworks through proposing human body-aware adaptation for biometrics.

## 2.3. Transfer Learning of Pre-trained Models

**Fine-tuning.** One of the most important problems in fine-tuning is overfitting by catastrophic forgetting [35]. To avoid

this problem, in Davoine *et al.* [36], an L2 loss in which fine-tuned and pre-trained parameters are forced to be close is proposed. Huan *et al.* [37] propose fine-tuning in which the similarity between feature vectors of the pre-trained and fine-tuned models is maintained. In Jin *et al.* [38], a subset of the source dataset is used for fine-tuning to avoid overfitting.

From the perspective of fine-tuning, our proposed method employs the regularization to avoid overfitting, as used in the previous methods [36, 37].

**Sample selection.** In active learning, samples that are informative for learning are selected to minimize annotation costs. The criteria of sample selection can be divided into uncertainty-based selection and diversity-based selection. The former considers the informativeness of each unlabeled sample for training, while the latter focuses on the dissimilarity between each unlabeled sample to avoid selecting similar samples.

For image classification, Li *et al.* [29] computes the entropy from the predicted image class probability and uses it as the uncertainty. In [30], for human pose estimation, uncertainty is computed from the pose heatmap. Yang *et al.* [31] propose an object detection-specific uncertainty that takes into account both classification and localization. Regarding diversity-based selection [39, 40], diverse samples are selected based on the mutual similarity between unlabeled samples. Core-set [39, 40] selects a representative subset of an unlabeled dataset that covers the whole distribution of the dataset.

Similar to these methods, our method also focuses on reducing annotation costs. Our method uses diversity-based selection, i.e., Core-set [39], as one component. On the other hand, uncertainty-based selection inevitably needs a model trained in a supervised manner, so it is not applicable to our method using a model pre-trained with no group activity annotation. Instead of the uncertainty-based selection, we propose query-aware video selection specialized for GARet.

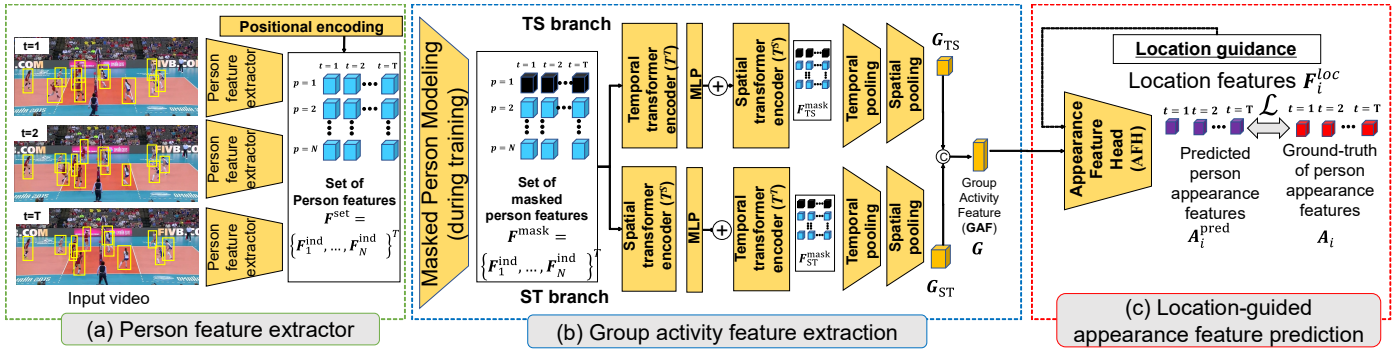


Figure 4: Overview of our group activity feature learning network. (a) Person feature extractor. The person feature is composed of appearance and location features. (b) Group Activity Feature Learning (GAFL) network. The GAF is learned from extracted people features. (c) Location-guided appearance feature prediction network with the GAF. The appearance feature of each person is predicted from the location feature of the person and the GAF extracted in (b). Through the appearance feature prediction, the GAF is learned in a self-supervised manner.

#### 2.4. Team Sports Scene Retrieval

Team sports scene retrieval is an important topic for team sports analysis, as proposed in [41, 42, 43, 44, 45, 46]. Early approaches [41, 42] describe each scene by the natural language representing the semantics of the scene (e.g., player A fails a free throw). While we can semantically retrieve a scene using the text as a query, it is challenging to perfectly represent the user’s desired scene by text. In trajectory-based retrieval [43, 44, 45, 46], on the other hand, scene similarity is computed by comparing the trajectories of multiple players. While real trajectories are used as a query in [43, 44, 46], Probst *et al* [45] propose to use a sketch-based query in which the users can represent their desired scene by drawing (e.g., drawing the trajectories of players). Liu *et al* [47] utilize visual features extracted from each video as a query for retrieval.

Similar to these methods, this paper also focuses on retrieval in team sports. However, our method focuses on human-in-the-loop adaptation of the pre-trained GAF for query videos provided by the users.

### 3. Proposed Method

Our method consists of the following two steps (Sec. 3.1 and Sec. 3.2, which are illustrated in Fig. 3 (A) and Fig. 3 (B), respectively).

In step (A), the GAF is pre-trained in a self-supervised manner [26] with a training set  $D^{\text{train}} = [D_1^{\text{train}}, \dots, D_{N^{\text{train}}}^{\text{train}}]$  where  $N^{\text{train}}$  denotes the number of training videos. Although the novelty of our method does not lie in step (A), Sec. 3.1 provides an overview of step (A), as our approach builds on the GAFL network pre-trained by step (A).

In step (B), which is proposed in this paper, the pre-trained GAFL network is updated to enhance the retrieval of the target group activity, represented by a few query videos (e.g., three) given by users only once. Group activity videos are retrieved from  $D^{\text{train}}$ , which is used as a video dataset. The GAFL network is updated with a few videos (e.g., five) selected from  $D^{\text{train}}$  using our proposed query-aware video selection for fine-tuning. Then, the users annotate the selected videos whether

or not the target group activity is observed. Using these annotated videos, metric learning is applied to the query videos to enhance the pre-trained GAF space with regularization for avoiding overfitting.

#### 3.1. Pre-training of GAFL network

**Person feature extractor (stage (a)).** As shown in Fig. 4 (a), the set of person features  $F_k^{\text{set}} \in \mathbb{R}^{T \times N \times C}$  are extracted from images of  $k$ -th video in  $D^{\text{train}}$ .  $F_k^{\text{set}}$  is composed of the  $C$ -dimensional features of  $N$  people obtained from  $T$  frames in the  $k$ -th video.  $F_{k,i}^{\text{ind}} \in \mathbb{R}^C$  is  $i$ -th person’s feature vector indicated by a blue cuboid in Fig. 4 (a).  $F_{k,i}^{\text{ind}}$  is obtained by the element-wise addition of appearance features (denoted by  $F_{k,i}^{\text{app}} \in \mathbb{R}^C$ ) and location features (denoted by  $F_{k,i}^{\text{loc}} \in \mathbb{R}^C$ ). The appearance feature  $F_{k,i}^{\text{app}}$  is obtained in three steps: (1) extracting a feature map from the whole image using VGG, (2) person feature map extraction from each person’s bounding box by using ROIAlign, and (3) feature map embedding into a  $C$ -dimensional vector via a linear transformation.  $F_{k,i}^{\text{loc}}$  is obtained by a spatial positional encoding of the center point of each person bounding box,  $(x, y)$ , as with [9].

**Group activity feature extraction (stage (b)).** To extract the features of people’s interactions from  $F_k^{\text{set}}$ , Masked Person Modeling (MPM) is applied to  $F_k^{\text{set}}$  to obtain  $F_k^{\text{mask}}$  during training. Given  $F_k^{\text{mask}}$ , the GAFL network consists of two branches (i.e., temporal-to-spatial (TS) and spatial-to-temporal (ST) branches) similar to [9].  $F_k^{\text{mask}}$  is independently fed into the TS and ST branches to acquire  $F_{k,TS}^{\text{mask}}$  and  $F_{k,ST}^{\text{mask}}$ , respectively. Then, both temporal and spatial max pooling are applied to  $F_{k,TS}^{\text{mask}}$  and  $F_{k,ST}^{\text{mask}}$  to obtain  $G_{k,TS} \in \mathbb{R}^C$  and  $G_{k,ST} \in \mathbb{R}^C$ , respectively. Finally,  $G_{k,TS}$  and  $G_{k,ST}$  are concatenated to obtain the final GAF  $G_k \in \mathbb{R}^{2C}$ .

**Location-guided appearance feature prediction (stage (c)).** During training,  $G_k$  is fed into the appearance feature head (denoted by AFH), as shown in Fig. 4 (c). In AFH, the appearance feature of each person (denoted by  $A_{k,i}^{\text{pred}} \in \mathbb{R}^{T \times R}$ ) is predicted from  $G_k$  with their location features (i.e.,  $F_{k,i}^{\text{loc}}$  extracted in stage (a)) as guidance.  $R$  is the dimension of the person appearance

---

**Algorithm 1:** Query-aware video selection (Sec. 3.2.1)

---

**Input:** Training set  $\mathbf{D}^{\text{train}}$  and Query set  $\mathbf{D}^{\text{query}}$   
**Output:**  $\mathbf{D}^{\text{ex}}$

```

1  $\mathbf{D}_{\text{ex}} \leftarrow \emptyset$  ;
2 for  $k = 1$  to  $N^{\text{query}}$  do
3    $H_k \leftarrow []$  ;
4   for  $k' = 1$  to  $|\mathbf{D}^{\text{train}}|$  do
5      $S_{k,k'} \leftarrow F_{\cos}(\mathbf{G}_k, \mathbf{G}_{k'})$  ;
6      $\tilde{S}_{k,k'} \leftarrow \frac{1}{P} \sum_p S_{k,k'}^p$  ;
7      $V_{k,k'} \leftarrow \frac{1}{P} \sum_p (S_{k,k'}^p - \tilde{S}_{k,k'})^2$  ;
8      $I_{k,k'} \leftarrow S_{k,k'} + \lambda V_{k,k'}$  ;
9     Append  $(I_{k,k'}, k')$  to  $H_k$  ;
10  end
11   $H_{\text{selected}} \leftarrow \text{TopK}(H_k, K = N^{\text{select}} * N^E)$  ;
12  for  $(I_{k,k'_{\text{selected}}}, k'_{\text{selected}})$  in  $H_{\text{selected}}$  do
13     $\mathbf{D}_{\text{ex}} \leftarrow \mathbf{D}_{\text{ex}} \cup \{\mathbf{D}_{k'_{\text{selected}}}^{\text{train}}\}$  ;
14     $\mathbf{D}^{\text{train}} \leftarrow \mathbf{D}^{\text{train}} \setminus \{\mathbf{D}_{k'_{\text{selected}}}^{\text{train}}\}$  ;
15  end
16 end
17 return  $\mathbf{D}_{\text{ex}}$  ;

```

---

features (i.e.,  $R = C$  in our method). The whole network is pre-trained in an end-to-end manner with a loss function as follows:

$$\mathcal{L}_{\text{paf}} = \frac{1}{N^{\text{train}} \cdot N} \sum_k^{\text{train}} \sum_i^N \mathcal{L}_{\text{MSE}}(\mathbf{A}_{k,i}^{\text{pred}}, \mathbf{A}_{k,i}) \quad (1)$$

$\mathcal{L}_{\text{paf}}$  is the mean squared loss function where  $\mathbf{A}_{k,i}$  denotes the appearance features extracted in stage (a) (i.e.,  $\mathbf{A}_{k,i} = \mathbf{F}_{k,i}^{\text{app}}$ ).

### 3.2. Human-in-the-loop adaptation of the pre-trained GAFL network

For the user-guided adaptation of the GAFL network,  $N^{\text{select}}$  videos are selected and given to the users for annotating these videos. In our method,  $N^{\text{select}} \times N^E$  videos are initially selected based on query-aware video selection as described in Sec. 3.2.1, diversity-aware video selection narrows down these videos to  $N^{\text{select}}$  videos as described in Sec. 3.2.2.  $N^E$ , where  $N^E \geq 1$ , denotes a coefficient to determine how many extra videos are given to diversity-aware video selection in order to select  $N^{\text{select}}$  diverse videos for efficiently GAFL fine-tuning.

#### 3.2.1. Query-aware video selection

Algorithm 1 shows the procedure of our query-aware video selection. Our query-aware video selection builds on the key idea that videos close to query videos in the GAF space are useful for fine-tuning. This is because these videos contain subtle distinctions between target and non-target group activities. Our query-aware video selection is defined by the following two criteria, i.e., query similarity and query local dissimilarity.

**Query similarity:** The query similarity is designed to select videos that are close to the query videos from  $\mathbf{D}^{\text{train}}$ . The query videos  $\mathbf{D}^{\text{query}} = [D_1^{\text{query}}, \dots, D_{N^{\text{query}}}^{\text{query}}]$ , in which the target group

---

**Algorithm 2:** Diversity-aware video selection (Sec. 3.2.2)

---

**Input:**  $\mathbf{D}^{\text{ex}}$   
**Output:** Selected videos  $\mathbf{D}^{\text{select}}$

```

1  $\mathbf{D}^{\text{select}} \leftarrow \{\text{Randomly select one video from } \mathbf{D}^{\text{ex}}\}$  ;
2  $\mathbf{D}^{\text{ex}} \leftarrow \mathbf{D}^{\text{ex}} \setminus \{D_1^{\text{select}}\}$  ;
3 for  $r = 1$  to  $N^{\text{select}} - 1$  do
4    $\mathbf{D}_r^{\text{select}} \leftarrow \mathbf{D}^{\text{select}}$  ;
5    $u \leftarrow \arg \max_{i \in \mathbf{D}^{\text{ex}}} (\min_{j \in \mathbf{D}_r^{\text{select}}} F_{\cos}(\mathbf{G}_i, \mathbf{G}_j))$  ;
6    $\mathbf{D}^{\text{select}} \leftarrow \mathbf{D}^{\text{select}} \cup \{D_u^{\text{ex}}\}$  ;
7    $\mathbf{D}^{\text{ex}} \leftarrow \mathbf{D}^{\text{ex}} \setminus \{D_u^{\text{ex}}\}$  ;
8 end
9 return  $\mathbf{D}^{\text{select}}$  ;

```

---

activity is observed, are provided by the users. Given a set of  $N^{\text{query}}$  query videos, each video in  $\mathbf{D}^{\text{train}}$  is scored by the GAF similarity with each query video as follows:

$$S_{k,k'} = F_{\cos}(\mathbf{G}_k, \mathbf{G}_{k'}) \quad (2)$$

where  $F_{\cos}(\mathbf{G}_k, \mathbf{G}_{k'})$  denotes the cosine similarity between the GAF of  $k$ -th query video and the GAF of  $k'$ -th video in  $\mathbf{D}^{\text{train}}$ , which are denoted by  $\mathbf{G}_k$  and  $\mathbf{G}_{k'}$ , respectively.  $\mathbf{G}_k$  and  $\mathbf{G}_{k'}$  are extracted by the pre-trained GAFL network (Sec. 3.1).

**Query local dissimilarity:** Several videos selected by our query similarity mentioned above may be too similar to each query video and not be informative for fine-tuning. To address this, selecting videos that are neither too high nor too low  $S_{k,k'}$  may be a straightforward approach, which leads to video selection from a wider distribution of videos. However, this approach still works only based on global similarity (i.e., the spatial configuration and visual features of all people). On the other hand, local dissimilarities represented by not all but several people are also essential to discriminate between target and non-target group activities. Such local dissimilarities may be neglected in global similarity evaluation using  $S_{k,k'}$ . Therefore, we also propose query local dissimilarity, focusing on selecting videos locally dissimilar to the query videos.

This query local dissimilarity is represented by the variation of GAFs extracted from partially masked people. First of all,  $N^V$  people are randomly masked in each query video and fed into the pre-trained GAFL network to obtain a Locally Masked GAF (LM-GAF). Then, the GAF similarities between the LM-GAF and GAFs extracted from all videos in  $\mathbf{D}^{\text{train}}$  are computed. A set of these GAF similarities is computed  $P$  times with different random masking patterns, where  $P$  is the number of patterns of masked people. The variance of the  $P$  GAF similarities computed from  $k'$ -th video in  $\mathbf{D}^{\text{train}}$  is regarded as an indicator of how much this video is locally dissimilar to the

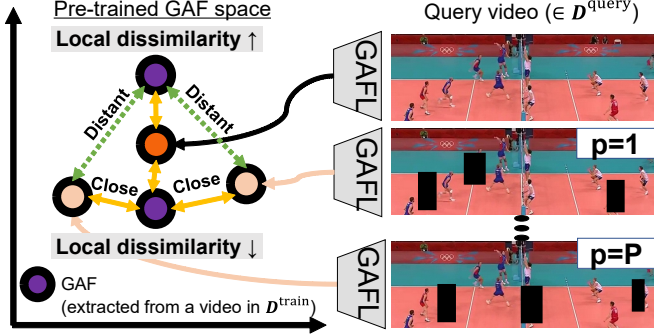


Figure 5: Query local dissimilarity computation. The query GAF and Locally Masked query GAF are extracted by the pre-trained GAFL network. For each video in  $D^{\text{train}}$ , the variance of the GAF similarities between the GAFs extracted from the query videos during the masking is computed.

$k$ -th query video, as follows:

$$V_{k,k'} = \frac{1}{P} \sum_p^P (S_{k,k'}^p - \bar{S}_{k,k'})^2 \quad (3)$$

$$\bar{S}_{k,k'} = \frac{1}{P} \sum_p^P S_{k,k'}^p, \quad (4)$$

where  $V_{k,k'}$  denotes the variance of the  $P$  GAF similarities between  $k$ -th query video and  $k'$ -th video in  $D^{\text{train}}$ .  $S_{k,k'}^p$ , where  $p \in \{1, \dots, P\}$ , denotes the GAF similarity between the  $p$ -th LM-GAF extracted from  $k$ -th query video and the GAF extracted from  $k'$ -th video in  $D^{\text{train}}$ .

Why can  $V_{k,k'}$  be regarded as a local dissimilarity score? If all people in two videos (i.e., a query video and a sample video) are almost the same with no local dissimilarity,  $V_{k,k'}$  becomes larger only due to the variation of LM-GAFs of a query video. On the other hand, if some people differ between the two videos, this difference makes  $V_{k,k'}$  much larger. Therefore,  $V_{k,k'}$  is regarded as the query local dissimilarity in our method.

**Query-aware similarity:** The query similarity (i.e.,  $S_{k,k'}$ ) and query local dissimilarity (i.e.,  $V_{k,k'}$ ) are ensembled to compute our informative score  $I_{k,k'}$ .  $I_{k,k'}$  indicates how informative  $k'$ -th video in  $D^{\text{train}}$  is for fine-tuning with respect to  $k$ -th query video as follows:

$$I_{k,k'} = S_{k,k'} + \lambda V_{k,k'}, \quad (5)$$

where  $\lambda$  is the weight to balance  $S_{k,k'}$  and  $V_{k,k'}$ .

For  $k$ -th query video, all videos in  $D^{\text{train}}$  are sorted in ascending order of  $I_{k,k'}$ . Then, the top  $N^{\text{select}} \times N^{\text{E}}$  videos are extracted for  $k$ -th query video. In total,  $N^{\text{select}} \times N^{\text{E}} \times N^{\text{query}}$  videos, denoted by  $D^{\text{ex}} = [D_1^{\text{ex}}, \dots, D_{N^{\text{select}} \times N^{\text{E}} \times N^{\text{query}}}^{\text{ex}}]$ , are extracted from all videos in  $D^{\text{train}}$ .

### 3.2.2. Diversity-aware video selection

While our query-aware video selection improves the GAFL fine-tuning efficiency, our method also uses Core-Set [39] to obtain a representative subset that covers the distribution of the entire set of samples for diversity. Using Core-Set,  $N^{\text{select}}$  videos

are selected from  $D^{\text{ex}}$ . The procedure of the diversity-aware video selection using Core-Set is shown in Algorithm 2.

According to Core-set, the first video (denoted by  $D_1^{\text{select}}$ ) is selected randomly from  $D^{\text{ex}}$ . The second and later videos are selected iteratively. The video selected in the  $r$ -th iteration is denoted by  $D_r^{\text{select}}$ . Given  $D_r^{\text{select}}$ , which is the set of selected videos by the  $r$ -th iteration,  $D_{r+1}^{\text{select}}$  is selected as follows:

$$D_{r+1}^{\text{select}} = D_u^{\text{ex}} \quad (6)$$

$$u = \arg \max_{i \in D^{\text{ex}}} \min_{j \in D_r^{\text{select}}} F_{\text{cos}}(\mathbf{G}_i, \mathbf{G}_j) \quad (7)$$

This video selection is looped  $N^{\text{select}}$  times to obtain  $D^{\text{select}} = [D_1^{\text{select}}, \dots, D_{N^{\text{select}}}^{\text{select}}]$ .

The users annotate these  $N^{\text{select}}$  videos in  $D^{\text{select}}$  as positive or negative for fine-tuning. While the binary annotation can be done by one user, we can apply multi-user annotation to improve the annotation quality. For example, more than one user is asked to annotate these  $N^{\text{select}}$  videos. Then, we can integrate the annotation results by multiple users in some way (e.g., majority voting) to improve the reliability of the annotation data.

### 3.2.3. Loss functions

In our fine-tuning, the pre-trained GAF space is updated with contrastive learning [48] using the positive and negative labels given to  $D^{\text{select}}$ , as mentioned at the beginning of Sec. 3.2. This contrastive learning is achieved with GAFs extracted from the query and selected videos. MSE loss to maintain the pre-trained GAF space is also applied to avoid overfitting as proposed in [37]. The whole network is fine-tuned in an end-to-end manner with the following loss function,  $\mathcal{L}$ , as follows:

$$\mathcal{L} = \mathcal{L}_{\text{ctr}} + \mathcal{L}_{\text{reg}} \quad (8)$$

$$\mathcal{L}_{\text{ctr}} = \frac{1}{N^{\text{query}}} \sum_k^N \max(0, d(\mathbf{G}_k, \mathbf{G}_{\text{pos}}) - d(\mathbf{G}_k, \mathbf{G}_{\text{neg}}) + \alpha) \quad (9)$$

$$\mathcal{L}_{\text{reg}} = \frac{1}{N^{\text{select}}} \sum_{k'}^N \mathcal{L}_{\text{MSE}}(\mathbf{G}_{k'}, \mathbf{G}_{k'}^{\text{pretrain}}) \quad (10)$$

$\mathcal{L}_{\text{ctr}}$  is the triplet loss function where  $\mathbf{G}_{\text{pos}}$  and  $\mathbf{G}_{\text{neg}}$  denote the GAFs extracted from positive and negative selected videos, respectively.  $d$  measures the Euclidean distance between two GAFs.  $\alpha$  denotes the margin.  $\mathcal{L}_{\text{reg}}$  is a regularization term designed to preserve the pre-trained GAF space.  $\mathbf{G}_{k'}^{\text{pretrain}}$  denotes the GAF extracted from the  $k'$ -th selected video with the pre-trained GAFL network before fine-tuning.

## 4. Experiments

### 4.1. Experimental protocols and evaluation metrics

Our experiments are designed to simulate a use case of the team-sports video retrieval task (described in Sec. 1) as mentioned in what follows.

Like query video selection by a user, query videos given at each trial in the experiments must be similar (i.e., must represent the same group activity). To guarantee that, we use

Table 1: Distribution of group activity classes annotated in the Volleyball dataset.

Group activity class	Number of labels
Right-set	644
Right-spike	623
Right-pass	801
Right-winpoint	295
Left-winpoint	367
Left-pass	826
Left-spike	642
Left-set	633

Table 2: Distribution of group activity classes annotated in the NBA dataset.

Group activity class	Number of labels
2p-succ.	961
2p-fail-off.	541
2p-fail-def.	1550
2p-layup-succ.	994
2p-layup-fail.-off	544
2p-layup-fail.-def	859
3p-succ.	911
3p-fail.-off	602
3p-fail.-def	2210

the group activity class annotations provided in team sports datasets for supervised GAR methods. Although the group activity classes annotated in the datasets are not fine-grained (e.g., spike, set, and pass in volleyball), we utilize them, as with experiments in supervised GAR methods. Specifically,  $N^{\text{query}}$  query videos in each retrieval trial are randomly sampled from videos of a single group activity class (denoted by  $C^q$ ) in a test set,  $\mathcal{D}^{\text{test}}$ . By our query-aware video selection using these  $N^{\text{query}}$  query videos,  $N^{\text{select}}$  videos in a training set,  $\mathcal{D}^{\text{train}}$ , are selected as proposed in Sec. 3.2. These selected videos in  $\mathcal{D}^{\text{train}}$  are also annotated with their group activity classes. Based on the annotated group activity classes in the datasets, we automatically generate binary annotations (i.e., 1 if the annotated group activity class matches  $C^q$ ) to simulate user annotations.

After fine-tuning the GAFL network with these query and selected videos with their annotated classes, the retrieval performance is evaluated on each query video as follows. From each query video, which is originally used as a query video for our query-aware video selection mentioned above, the nearest  $K$  videos in the finetuned GAF space are retrieved from a training set,  $\mathcal{D}^{\text{train}}$ . Then, Precision@K, expressed by  $\frac{N^P}{K}$  where  $N^P$  denotes the number of retrieved videos that are correctly classified to  $C^q$ , is evaluated. Since  $N^{\text{select}}$  videos in  $\mathcal{D}^{\text{train}}$  are used in the fine-tuning, we use  $K$ , which is large enough compared with  $N^{\text{select}}$  to evaluate a retrieval performance on videos not used in the fine-tuning. We also evaluate Hit@K, as used in [49, 1], in which the retrieval is regarded as success (i.e., Hit@K=1) if at least one retrieved video is classified to  $C^q$ . Otherwise, Hit@K=0. Hit@K is also suitable to simulate a use case in the team sports retrieval task; team sports analysts may need

Table 3: Distribution of group activity classes annotated in the Collective Activity dataset.

Group activity class	Number of labels
Moving	1111
Waiting	455
Queuing	502
Talking	450

only one target group activity video among all retrieved videos because the analysts can easily find what they need from the retrieved videos (e.g., three videos) than from all training videos (e.g., thousands of videos).

In experiments in this paper, the main task is to enhance the performance of retrieval using the original query videos. Evaluation metrics with the original query videos are called “Precision@K original” and “Hit@K original.” In addition, we also evaluate retrieval using queries sampled from all other test videos (i.e., “Precision@K others” and “Hit@K others”). This evaluation using the other test videos validates the generalizability of our fine-tuning.

The aforementioned evaluation process is repeated 10 times in each group activity class independently. That is, in each evaluation process, fine-tuning begins with the original pre-trained model.

#### 4.2. Datasets

The following two datasets of team sports (i.e., Volleyball and NBA datasets) are used to validate the retrieval performance in our experiments. To further validate the applicability of our method, we also use the Collective activity dataset as a non-sports dataset.

**Volleyball dataset** [27] consists of 4,830 videos extracted from 55 games. The 4,830 videos are divided into 3,493 train and 1,337 test sets. Each video is annotated with one of the predefined eight group activity classes, i.e., Left-spike, Right-spike, Left-set, Right-set, Left-pass, Right-pass, Left-winpoint, and Right-winpoint. The detailed information about the group activity annotation data is summarized in Table 1. The group activity classes are manually annotated for each video clip. The annotation process is reliable because the annotators can confirm each video, not an image. While each video has 41 frames, its center frame, nine frames before the center, and ten frames after the center (20 frames, in total) have annotations with the full-body bounding boxes of all players and their action classes, i.e., Waiting, Setting, Digging, Falling, Spiking, Jumping, Moving, Blocking, and Standing.

**NBA Dataset (NBA)** [14] comprises 9,172 sequences extracted from 181 professional basketball matches. These sequences are partitioned into a training set of 7,624 sequences and a test set of 1,548 sequences. Each sequence is annotated with one of nine pre-defined group activity classes, including: 2p-succ., 2p-fail.-off., 2p-fail.-def., 2p-layup-succ., 2p-layup-fail.-off., 2p-layup-fail.-def., 3p-succ., 3p-fail.-off., and 3p-fail.-def. Table 2 shows the detailed class distribution in the NBA dataset. The group activity classes are annotated from game logs provided by the

Table 4: Quantitative comparison of retrieval on the VolleyBall Dataset (Volleyball). The best result in each column is colored in red. In “Ours”, the whole network is fine-tuned for each target group activity with five selected videos for fine-tuning. As query videos, three videos are sampled from the test videos for each fine-tuning. The retrieval results are the weighted average of eight group activity classes, considering the number of videos in each group activity class.

	Precision@5 original	Precision@10 original	Precision@5 others	Precision@10 others	Hit@5 original	Hit@10 original	Hit@5 others	Hit@10 others
B1-Compact128 [1]	0.318	0.299	0.315	0.293	0.737	0.870	0.761	0.900
B2-VGG19 [1]	0.319	0.291	0.322	0.297	0.791	0.905	0.777	0.907
HRN [1]	0.280	0.254	0.276	0.262	0.728	0.861	0.728	0.881
GAFL [26]	0.557	0.533	0.557	0.535	0.886	0.962	0.881	0.936
Ours	<b>0.739</b>	<b>0.647</b>	<b>0.596</b>	<b>0.564</b>	<b>0.988</b>	<b>0.993</b>	<b>0.905</b>	<b>0.950</b>

NBA’s official website. Since abnormal annotations are manually filtered after the initial annotation, the annotation process is reliable, as with the Volleyball dataset. Unlike the Volleyball dataset, each sequence consists of 72 frames, thereby capturing long-term group activity behaviors.

**Collective Activity Dataset (CAD)** [13] consists of 44 videos. Every ten frames are annotated with people’s bounding boxes and their action classes. Each person’s action classes are annotated from either of NA, Crossing, Waiting, Queuing, Walking, or Talking. Different from the Volleyball and NBA datasets, group activity class is determined by the large number of person actions in a frame. The detailed distribution of group activity classes is shown in Table 3. As the person action classes are manually annotated by confirming the target and the neighboring frames, we can say that the group activity classes obtained from the person action classes are reliable. For further annotation quality control, we merge Crossing and Walking into Moving due to the high similarity between Crossing and Walking classes, as with [7, 50].

#### 4.3. Training Details

**Pre-training (step (A) in Fig. 3):** Our network is optimized by Adam [51] with  $\beta_1 = 0.9$ ,  $\beta_2 = 0.999$ , and  $\epsilon = 10^{-8}$ . The learning rate is 0.0001. In all datasets, the whole image is resized to 320x640. We employ the VGG-19 models as a person feature extractor (Fig. 4 (a)). Our AFH consists of three fully-connected layers.

**Fine-tuning (step (B) in Fig. 3):** In our human-in-the-loop adaptation, our network is also optimized by Adam  $\beta_1 = 0.9$ ,  $\beta_2 = 0.999$ , and  $\epsilon = 10^{-8}$  with the same parameters as the pre-training stage. The margin  $\alpha$  in contrastive learning is set to 10.  $N^{\text{query}} = 3$  and  $N^{\text{select}} = 5$  in our experiments. In all datasets,  $N^E = 4$  and  $N^V = 2$  are used in our proposed query-aware video selection (Sec. 3.2.1).

#### 4.4. Comparative Experiments

Based on the experimental protocols and evaluation metrics (Sec. 4.1), we compare our method with several methods on the Volleyball and NBA datasets as described in Sec. 4.2. In this section, we comprehensively compare these methods through qualitative and quantitative experiments for each dataset.

Our method is compared with two baseline methods shown in [1] and two SOTA methods [1, 26]. In the two baseline methods and [1], the set of person features (i.e., the concatenation of

$\mathbf{F}_{\text{TS}}^{\text{mask}}$  and  $\mathbf{F}_{\text{ST}}^{\text{mask}}$  in Fig. 4 (b)) is used for retrieval, while  $\mathbf{G}$  is used in GAFL [26] and our method. The essential difference between our method and all the others is that our method fine-tunes the GAF model in a human-in-the-loop manner.

**Volleyball dataset.** Table 4 shows that our method significantly improves the retrieval performance. We can see that the retrieval results are improved not only for the original query videos used for fine-tuning but also for the other videos.

Figure 6 shows visual retrieval results. In each row of the left column, a middle frame of each query video is shown. In the center and right columns, the middle frames of videos retrieved by GAFL and our method (i.e., fine-tuned GAFL) are shown, respectively.

In the upper example, our method successfully retrieves “L-winpoint,” while GAFL [26] retrieves “R-pass.” This difference can be interpreted as our method learns the characteristic configuration of people on the left side (i.e., people are celebrating a point in a circle). The middle example also shows that our method emphasizes people related to the spike group activity (e.g., spiking and blocking person actions) in the GAF during fine-tuning. In the bottom example, GAFL [26] incorrectly retrieves “L-set” from “L-pass” query videos. This failure result may come from the similar configurations of people between the query and the retrieved videos. That is, there are three people who are standing in front of the net on the right side in both the query video and the video retrieved by GAFL. Different from GAFL, our method correctly retrieves “L-pass.” This result indicates that our proposed video selection process selects various L-pass videos with different people configurations for fine-tuning.

Retrieval results on each group activity are shown in Table 5. We can see that our method works well in all group activities. These results validate that our proposed fine-tuning can be generalized for any group activity.

Figure 7 shows the GAFs extracted from the query and selected videos visualized by t-SNE [28] on the Volleyball dataset. The GAF space is fine-tuned for “L-set.” The GAFs extracted from the query and selected videos are visualized with the middle frame of each video. Compared to GAFL [26], “Ours” successfully projects three selected videos annotated as target group activity (indicated by green points) closer to the query videos.

Figure 8 shows the learned GAF spaces on the Volleyball dataset. Different from Fig. 7, GAFs extracted from all videos



Figure 6: Comparison of GAF on the Volleyball dataset. In all examples, the middle frame of the video is shown for visualization. In each image, manually annotated group activity labels are visualized in the bottom right side of each image.

Table 5: Detailed analysis of retrieval on the Volleyball Dataset. The retrieval results using Precision@10 (original) for each group activity class are shown in the corresponding column. The best result in each column is colored in red.

Metric = Precision@10 (original)	L-spike	L-pass	L-set	L-winpoint	R-spike	R-pass	R-set	R-winpoint
B1-Compact128 [1]	0.320	0.243	0.357	0.330	0.307	0.340	0.260	0.223
B2-VGG19 [1]	0.333	0.230	0.310	0.283	0.283	0.360	0.267	0.233
HRN [1]	0.233	0.257	0.217	0.300	0.250	0.363	0.190	0.197
GAFL [26]	0.763	0.393	0.557	0.473	0.777	0.467	0.450	0.303
Ours	<b>0.837</b>	<b>0.493</b>	<b>0.683</b>	<b>0.617</b>	<b>0.817</b>	<b>0.613</b>	<b>0.597</b>	<b>0.473</b>

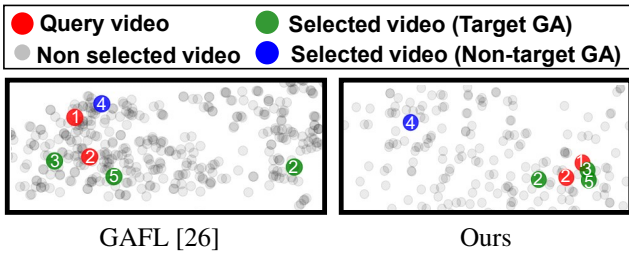


Figure 7: Visualization of GAFs extracted from the query and selected videos by t-SNE. The target group activity is “L-set” in this figure. In this GAF visualization, indices of the query and selected videos are shown in each corresponding GAF. While we utilize three query videos and five selected videos in our experiments, we display only two query videos and four selected videos due to space constraints.

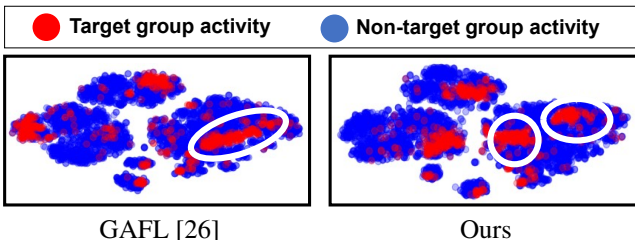


Figure 8: Visualization of learned GAF space by t-SNE on the Volleyball dataset. The target group activity is “L-set” in this figure.

Table 6: Quantitative comparison of retrieval on the NBA Dataset. The best result in each column is colored in red. In “Ours”, the whole network is fine-tuned for each target group activity with five selected videos. As query videos, three videos are sampled from the test videos for each fine-tuning.

	Precision@10 original	Hit@10 original
B1-Compact128 [1]	0.161	0.749
B2-VGG19 [1]	0.156	0.776
HRN [1]	0.135	0.771
GAFL [26]	0.206	0.798
Ours	<b>0.233</b>	<b>0.839</b>

in  $D^{test}$  are visualized in this figure. We can see that the GAFs of the target group activity videos (indicated by red points) are distributed widely in GAFL [26], as shown in the white circle. Compared to this GAF space of GAFL, in the GAF space fine-tuned by our method, the GAFs of the target group activity videos are projected within smaller regions as enclosed by the two white circles. The results indicate that our fine-tuning generally updates the GAF space to improve discriminativity for the target group activity in all videos in  $D^{test}$ , as also proved by “Precision@K others” and “Hit@K others” in Table 4.

**NBA dataset.** The comparison of GARet on the NBA dataset is shown in Table 6. Table 6 shows that our method is the best in all metrics on the NBA dataset. These results demonstrate the generalization ability of our method across various team sports, which differ in terms of the number of people and the granularity of target group activities.

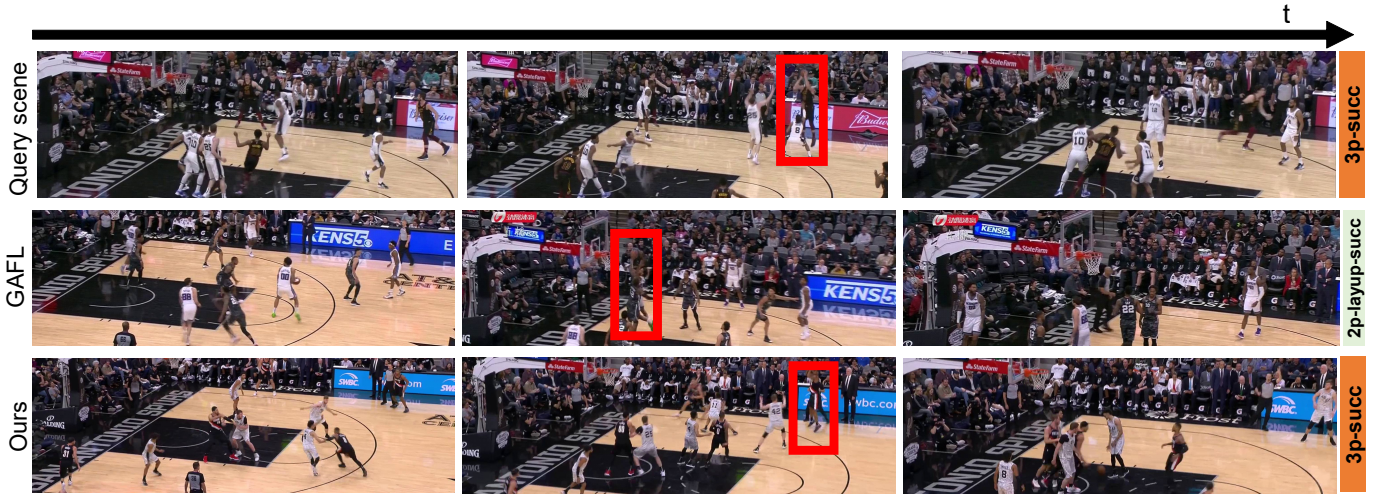


Figure 9: Comparison of GARet on the NBA dataset. A shooter is enclosed by a red rectangle in the images. In each example, manually annotated group activity labels are visualized on the rightmost side.

Table 7: Quantitative comparison of retrieval on the Collective Activity Dataset. The best and second-best results in each column are colored in red and blue. In “Ours”, the whole network is fine-tuned for each target group activity with five selected videos. As query videos, three videos are sampled from the test videos for each fine-tuning.

	Precision@ 10 original	Hit@ 10 original
B1-Compact128 [1]	0.799	0.925
B2-VGG19 [1]	0.660	0.901
HRN [1]	0.522	0.859
GAFL [26]	0.788	0.840
Ours	0.814	0.866

Figure 9 shows visual retrieval results on the NBA dataset. In the upper row, the query videos used for retrieval are shown with their group activity labels. In the second and third rows, videos retrieved by GAFL [26] and our method are shown with their group activity labels, respectively. A shooter is enclosed by a red rectangle in the images. In this example, the video annotated as 3p-succ activity is used as the query. While the video in which 2p-layup-succ activity is observed is retrieved by GAFL [26], our method successfully retrieves the video in which 3p-succ activity is observed.

**Collective Activity Dataset.** In addition to validating the two sports datasets, which is the main focus of this work, we also conduct experiments on the Collective Activity Dataset. This dataset includes general living scenes and can be used to validate the generality of our method.

Table 7 shows the comparison of GARet on the Collective Activity Dataset. In the experiments on this dataset, we empirically decided to remove  $\mathcal{L}_{reg}$  from  $\mathcal{L}$ . We can see that our method is best in “Precision@10 original” in Table 7. These results demonstrate that GARet by our method is applicable to non-sports videos. While “B1-Compact128” is better than “Ours” in Hit@10 original, the result in our method is cer-

Table 8: Comparison of video selection on the Volleyball dataset. The best result in each column is colored in red.

	Precision@ 10 original	Hit@ 10 original
Random	0.565	0.546
K-means [40]	0.568	0.550
Core-set [39]	0.560	0.543
Ours w/o $\mathbf{S}$	0.566	0.545
Ours w/o $\mathbf{V}$	0.640	0.562
Ours	0.647	0.564

tainly improved from the result in the pre-trained model (i.e., GAFL [26]). The performance gap can be filled with improvements in the pre-trained models.

#### 4.5. Detailed analysis

##### 4.5.1. Comparison of video selection

To validate the effectiveness of our proposed video selection, we compare the retrieval results with GAF models fine-tuned by videos selected using the following five other methods, as shown in Table 8. In “Random,” videos are randomly selected from  $\mathbf{D}^{train}$ . In “Core-set” and “K-means,” GAFs extracted by the pre-trained GAFL network are used for each method. In “Ours w/o  $\mathbf{S}$ ” and “Ours w/o  $\mathbf{V}$ ,”  $\mathbf{S}$  and  $\mathbf{V}$  are removed from  $\mathbf{I}$  (shown in Eq. 5), respectively.

The results validate that our method is best in all metrics. Compared with “Core-set” and “K-means” to our method, our method is significantly better (i.e., while Precision@10 (original) is 0.560 and 0.568 in “Core-set” and “K-means”, it is 0.647 in our method). These results indicate that our proposed query-aware video selection for selecting valuable videos is effective compared to other data selections in this fine-tuning. Furthermore, the performance gain of “Ours” from “Ours w/o  $\mathbf{V}$ ” demonstrated that query local dissimilarity contributes to video

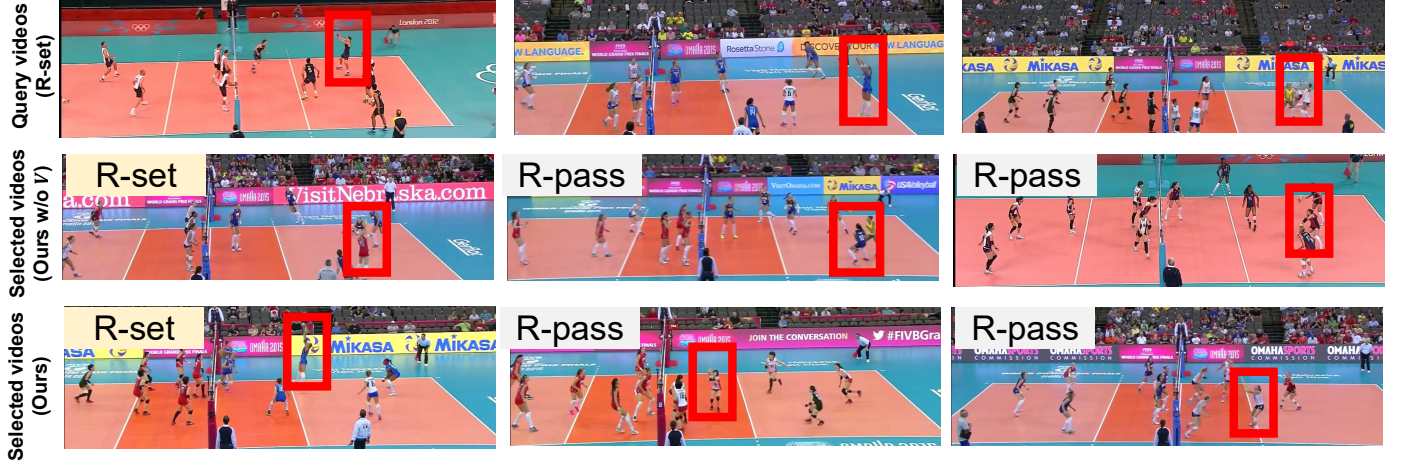


Figure 10: Examples of videos selected in “Ours w/o  $V$ ” and “Ours” when the queries are R-set videos. The upper row shows the query videos. In the second and third rows, the videos selected by “Ours w/o  $V$ ” and “Ours” are shown with their manually annotated group activity labels, respectively. A receiving player is enclosed by a red rectangle in the images. Due to space limitations, only three videos are displayed from the selected  $N^{\text{select}}$  videos.

selection. The results demonstrated that the motivation of  $V$  (i.e., selecting videos locally dissimilar to the query videos) is important to learn discriminative features. We can also see the performance gain from “Ours w/o  $S$ .” This result validates that query similarity (i.e.,  $S$ , as defined in Eq. 2) in our method improves the retrieval performance of target group activity. Since  $S$  is proposed for selecting videos globally similar to the query videos, the results indicate that selecting globally similar videos to the query videos is important for this fine-tuning in addition to selecting the local dissimilar videos by  $V$ , as defined in Eq. 4.

#### 4.5.2. Example of selected videos

Figure 10 shows the example of videos selected in “Ours” and “Ours w/o  $V$ ” when the queries are R-set videos on the Volleyball dataset. While both “Ours” and “Ours w/o  $V$ ” select videos in which a ball is received by a player (enclosed by a red rectangle), their locations are different. In “Ours w/o  $V$ ,” the location of the player receiving the ball in each video is similar (i.e., the player is located on the rear side of the right court). Unlike “Ours w/o  $V$ ,” “Ours” selects videos where the receiving player is located in various areas on the court. Using the selected videos in which players receive the ball in different locations, “Ours” efficiently learns the GAF discriminative for the R-set group activity.

#### 4.5.3. Analysis of query-aware video selection

**Effect of  $N^V$ .** Figure 11 shows the retrieval performance changes depending on  $N^V$  (i.e., the number of masking people) in query local dissimilarity (Sec. 3.2.1) on the Volleyball dataset. In this figure,  $N^V$  is increased from 1 to 6 in increments of 1. We can see that the best result is obtained with  $N^V = 2$ , and the results significantly drop with  $N^V > 5$ . These results validate that masking using a small number of people is effective in our query local dissimilarity.

**Effect of  $N^E$ .** As mentioned in Sec. 3.2.1,  $N^E$  controls the number of videos selected in our query-aware video selection



Figure 11: Retrieval performance changes depending on  $N^V$  in query local dissimilarity on the Volleyball dataset.  $N^V$  is increased from 1 to 6 in increments of 1. Retrieval results evaluated by Precision@10 (original) are shown in this figure.

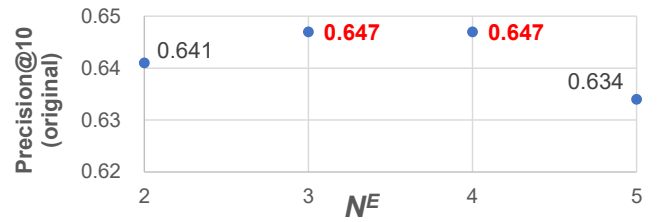


Figure 12: Retrieval performance changes depending on  $N^E$  in query-aware video selection on the Volleyball dataset.  $N^E$  is increased from 2 to 5 in increments of 1. Retrieval results evaluated by Precision@10 (original) are shown in this figure.

before diversity-aware video selection described in Sec. 3.2.2. Figure 12 shows that the retrieval performance changes on the Volleyball dataset when  $N^E$  is changed from 2 to 5 in increments of 1. We can see that the best results are obtained when  $N^E = 3, 4$ . Furthermore, we can see that the retrieval performance is largely dropped with  $N^E = 5$  (i.e., 0.647 in  $N^E = 4$  drops to 0.634 in  $N^E = 5$ ). The results validate that selecting videos far from the query videos in the pre-trained GAF space degrades the retrieval performance.

## 5. Concluding Remarks

This paper proposed a human-in-the-loop adaptation in the pre-trained GAFL for team sports video retrieval. The pre-trained GAFL is updated for the target group activity presented by query videos given by users. In addition, query-aware video selection specialized for GARet is also proposed for data efficiency to reduce users’ annotations. While weak supervision (i.e., positive and negative labeling to selected videos) is additionally required compared with the fully-unsupervised baseline [26], our proposed human-in-the-loop adaptation significantly improves the retrieval performance on two team sports datasets (e.g., the performance gain is 0.114 in Precision@10 original compared “Ours” with GAFL [26] on the Volleyball dataset).

Future research directions to further decrease annotation costs include explicitly identifying key people of the target group activity, which is implicitly learned from a large number of videos.

## References

- [1] M. S. Ibrahim, G. Mori, Hierarchical relational networks for group activity recognition and retrieval, in: ECCV, 2018.
- [2] J. Wu, L. Wang, L. Wang, J. Guo, G. Wu, Learning actor relation graphs for group activity recognition, in: CVPR, 2019.
- [3] S. M. Azar, M. G. Atigh, A. Nickabadi, A. Alahi, Convolutional relational machine for group activity recognition, in: CVPR, 2019.
- [4] R. R. A. Pramono, Y. Chen, W. Fang, Empowering relational network by self-attention augmented conditional random fields for group activity recognition, in: ECCV, 2020.
- [5] M. Ehsanpour, A. Abedin, F. S. Saleh, J. Shi, I. D. Reid, H. Rezatofighi, Joint learning of social groups, individuals action and sub-group activities in videos, in: ECCV, 2020.
- [6] K. Gavrilyuk, R. Sanford, M. Javan, C. G. M. Snoek, Actor-transformers for group activity recognition, in: CVPR, 2020.
- [7] H. Yuan, D. Ni, M. Wang, Spatio-temporal dynamic inference network for group activity recognition, in: ICCV, 2021.
- [8] S. Li, Q. Cao, L. Liu, K. Yang, S. Liu, J. Hou, S. Yi, Groupformer: Group activity recognition with clustered spatial-temporal transformer, in: ICCV, 2021.
- [9] M. Han, D. J. Zhang, Y. Wang, R. Yan, L. Yao, X. Chang, Y. Qiao, Dual-ai: Dual-path actor interaction learning for group activity recognition, in: CVPR, 2022.
- [10] M. Tamura, R. Vishwakarma, R. Vennelakanti, Hunting group clues with transformers for social group activity recognition, in: ECCV, 2022.
- [11] H. Zhou, A. Kadav, A. Shamsian, S. Geng, F. Lai, L. Zhao, T. Liu, M. Kapadia, H. P. Graf, COMPOSER: compositional reasoning of group activity in videos with keypoint-only modality, in: ECCV, 2022.
- [12] D. Kim, J. Lee, M. Cho, S. Kwak, Detector-free weakly supervised group activity recognition, in: CVPR, 2022.
- [13] W. Choi, K. Shahid, S. Savarese, What are they doing? : Collective activity classification using spatio-temporal relationship among people, in: ICCVW, 2009.
- [14] R. Yan, L. Xie, J. Tang, X. Shu, Q. Tian, Social adaptive module for weakly-supervised group activity recognition, in: ECCV, 2020.
- [15] C. Nakatani, K. Sendo, N. Ukita, Group activity recognition using joint learning of individual action recognition and people grouping, in: MVA, 2021.
- [16] Z. Xie, T. Gao, K. Wu, J. Chang, An actor-centric causality graph for asynchronous temporal inference in group activity, in: CVPR, 2023.
- [17] R. Yan, L. Xie, J. Tang, X. Shu, Q. Tian, Higcin: Hierarchical graph-based cross inference network for group activity recognition, IEEE Trans. Pattern Anal. Mach. Intell. 45 (6) (2023) 6955–6968.
- [18] Z. Li, X. Chang, Y. Li, J. Su, Skeleton-based group activity recognition via spatial-temporal panoramic graph, in: ECCV, 2024.
- [19] D. Kim, Y. Song, M. Cho, S. Kwak, Towards more practical group activity detection: A new benchmark and model, in: ECCV, 2024.
- [20] Y. Zhang, W. Liu, D. Xu, Z. Zhou, Z. Wang, Bi-causal: Group activity recognition via bidirectional causality, in: CVPR, 2024.
- [21] M. A. Nugroho, S. Woo, S. Lee, J. Park, Y. Wang, D. Kim, C. Kim, Flow-assisted motion learning network for weakly-supervised group activity recognition, in: ECCV, 2024.

- [22] A. M. S. Vincent Omollo Nyangaresi, Smart wearables powered by ai transforming human activity recognition, *Babylonian Journal of Artificial Intelligence* 2024 (2024) 128–133.
- [23] R. B. Foster, *American Football Playbook: 210 Field Templates*, Createspace Independent Pub, 2016.
- [24] D. Monjes, G. Salas, *American Football playbook: Coach or players can draw plays in half field diagrams with notes section*, Independently, 2021.
- [25] F. Team, Nfl playbooks archives, Online, accessed: 2025-03-04 (2018).
- [26] C. Nakatani, H. Kawashima, N. Ukita, Learning group activity features through person attribute prediction, in: *CVPR*, 2024.
- [27] M. S. Ibrahim, S. Muralidharan, Z. Deng, A. Vahdat, G. Mori, A hierarchical deep temporal model for group activity recognition, in: *CVPR*, 2016.
- [28] L. Van der Maaten, G. Hinton, Visualizing data using t-sne., *Journal of machine learning research* 9 (11) (2008).
- [29] X. Li, Y. Guo, Adaptive active learning for image classification, in: *CVPR*, 2013.
- [30] H. Taketsugu, N. Ukita, Active transfer learning for efficient video-specific human pose estimation, in: *WACV*, 2024.
- [31] C. Yang, L. Huang, E. J. Crowley, Plug and play active learning for object detection, in: *CVPR*, 2024.
- [32] Z. Li, X. Chang, Y. Li, J. Su, Skeleton-based group activity recognition via spatial-temporal panoramic graph, in: *ECCV*, 2024.
- [33] A. Vaswani, N. Shazeer, N. Parmar, J. Uszkoreit, L. Jones, A. N. Gomez, L. Kaiser, I. Polosukhin, Attention is all you need, in: *NIPS*, 2017.
- [34] H. M. S. Kassim Mohammed Awad, Lamia Faris Tulaib, Gait recognition by computing fixed body parameters, *Babylonian Journal of Networking* 2024 (2024) 191–197.
- [35] T. Zhang, F. Wu, A. Katiyar, K. Q. Weinberger, Y. Artzi, Revisiting few-sample BERT fine-tuning, in: *CLR*, 2021.
- [36] X. Li, Y. Grandvalet, F. Davoine, Explicit inductive bias for transfer learning with convolutional networks, in: J. G. Dy, A. Krause (Eds.), *ICML*, 2018.
- [37] X. Li, H. Xiong, H. Wang, Y. Rao, L. Liu, J. Huan, Delta: Deep learning transfer using feature map with attention for convolutional networks, in: *ICLR*, 2019.
- [38] Z. Liu, Y. Xu, Y. Xu, Q. Qian, H. Li, X. Ji, A. B. Chan, R. Jin, Improved fine-tuning by better leveraging pre-training data, in: *NeurIPS*, 2022.
- [39] O. Sener, S. Savarese, Active learning for convolutional neural networks: A core-set approach, in: *ICLR*, 2018.
- [40] F. Zhdanov, Diverse mini-batch active learning, *arXiv* abs/1901.05954 (2019).
- [41] C. Xu, Y. Zhang, G. Zhu, Y. Rui, H. Lu, Q. Huang, Using webcast text for semantic event detection in broadcast sports video, *IEEE Trans. Multim.* 10 (7) (2008) 1342–1355.
- [42] C. Chen, L. Chen, A novel approach for semantic event extraction from sports webcast text, *Multim. Tools Appl.* 71 (3) (2014) 1937–1952.
- [43] Z. Wang, C. Long, G. Cong, C. Ju, Effective and efficient sports play retrieval with deep representation learning, in: *ACM SIGKDD*, 2019.
- [44] Z. Wang, C. Long, G. Cong, Similar sports play retrieval with deep reinforcement learning, *IEEE Trans. Knowl. Data Eng.* 35 (4) (2023) 4253–4266.
- [45] L. Probst, I. A. Kabary, R. Lobo, F. Rauschenbach, H. Schuldt, P. Seidenschwarz, M. Rumo, Sportsense: User interface for sketch-based spatio-temporal team sports video scene retrieval, in: *IUI*, 2018.
- [46] M. Di, D. Klabjan, L. Sha, P. Lucey, Large-scale adversarial sports play retrieval with learning to rank, *ACM Trans. Knowl. Discov. Data* 12 (6) (2018) 69:1–69:18.
- [47] H. Liu, H. Zhang, A content-based broadcasted sports video retrieval system using multiple modalities: Sportbr, in: *CIT*, 2005.
- [48] T. Chen, S. Kornblith, M. Norouzi, G. E. Hinton, A simple framework for contrastive learning of visual representations, in: *ICML*, 2020.
- [49] K. Yi, X. Shen, Y. Gou, M. Elhoseiny, Exploring hierarchical graph representation for large-scale zero-shot image classification, in: *ECCV*, 2022.
- [50] M. Wang, B. Ni, X. Yang, Recurrent modeling of interaction context for collective activity recognition, in: *CVPR*, 2017.
- [51] D. P. Kingma, J. Ba, Adam: A method for stochastic optimization, in: Y. Bengio, Y. LeCun (Eds.), *ICLR*, 2015.